

Detection of Soliton Shape Modes in Polyacetylene

Z. Vardeny, E. Ehrenfreund, and O. Brafman

Physics Department and Solid State Institute, Technion-Israel Institute of Technology, Haifa 32000, Israel

B. Horovitz

Department of Physics, Ben-Gurion University, Beer-Sheva 84105, Israel

and

H. Fujimoto, J. Tanaka, and M. Tanaka

*Department of Chemistry, Faculty of Science and College of General Education,
Nagoya University, Chikusa, Nagoya 464, Japan*

(Received 26 June 1986)

We observed soliton shape modes by photoinduced absorption in partially isomerized $(\text{CH})_x$ and $(\text{CD})_x$, coexisting with the soliton translational modes. The shape modes' ir activity, their dependence on the degree of isomerization, and the photoinduced spectra are explained in detail by a symmetry-breaking interaction which allows coupling of shape modes and translational modes. We also observed soliton shape-mode absorption in fully isomerized samples as phonon sidebands associated with optical transitions of neutral solitons above 1.5 eV.

PACS numbers: 72.80.Le, 72.40.+w, 78.50.-w

Nonlinear excitations in quasi one-dimensional systems have become in recent years the subject of considerable interest.¹⁻⁵ Essential information on these excitations is contained in their small-oscillation spectra. In particular, solitons in a dimerized Peierls condensate were predicted¹ to have three types of independent linear modes: translational and shape modes, which are localized at the soliton site, and extended modes. The translational (T) mode is an odd-symmetry Goldstone mode which arises because of the breaking of translational symmetry by the presence of the soliton. The even-symmetry shape (S) mode describes a modification of the form of the soliton. Finally, the extended modes have a continuum spectrum similar to that of phonons in the absence of solitons. More recent calculations² have shown an additional weaker odd-symmetry mode (g_3) with frequency higher than the S mode.

The implications of these ideas for solitons in polyacetylene, $(\text{CH})_x$, has turned out to be unexpectedly elegant.¹⁻⁵ It has been recognized that $(\text{CH})_x$ has three normal modes which couple to the dimerization, and the generalization of the one-component theory was readily achieved.^{3,5} The three strongly coupled phonons of the solitonless chain with even symmetry have been shown⁶ to be amplitude modes of the dimerization gap. The T modes of the charged soliton (S^\pm) are ir active³ with very intense oscillator strength due to an efficient coupling⁷ to the charges trapped at the defect site. The soliton T modes were therefore extensively studied by ir absorption of S^\pm introduced onto the chain by either doping or photoexcitation.^{6,8,9} The soliton shape modes, however, are more difficult to detect since they are not ir active even for^{2,5} S^\pm , and their Raman-scattering inten-

sity is probably too weak to detect in the presence of the much stronger scattering intensity from the extended amplitude modes. Therefore, no experimental study of the S modes is available and an essential link with soliton theories¹⁻⁵ is missing.

In the present work we report the detection of soliton S modes by use of the photoinduced absorption (PA) technique. The S modes are observed in partially isomerized samples as additional ir-active modes associated with the photoinduced S^\pm . These additional modes gradually disappear upon dimerization and in fully isomerized samples we observe only T modes. These results are explained by a symmetry-breaking interaction in the partially isomerized samples which lifts the ground-state degeneracy of the *trans* structure. Consequently, the soliton defects break inversion symmetry and an interaction between the S and T modes is possible. The soliton S modes are also identified in the photo-modulation spectrum of the neutral soliton (S^0) defects as phonon sidebands.

Steady-state PA was generated by an Ar^+ laser beam chopped at 140 Hz; the changes (ΔT) in the sample transmission T were measured with an incandescent light source. $\Delta T/T$ is proportional to the change $\Delta\alpha$ in the absorption coefficient α . The samples were thin films of $(\text{CH})_x$ and $(\text{CD})_x$ (~ 1000 Å thick) polymerized on KBr substrate. The as-grown films, denoted $t(c)$, contained 70% *cis* and 30% *trans* as determined by Raman spectroscopy.¹⁰ Measurements on *trans* samples were done on the same films after isomerization for 30 min at 180 °C; the complete isomerization was verified by resonant Raman scattering.¹¹

In Fig. 1 the photoinduced absorption ($-\Delta T/T$) at

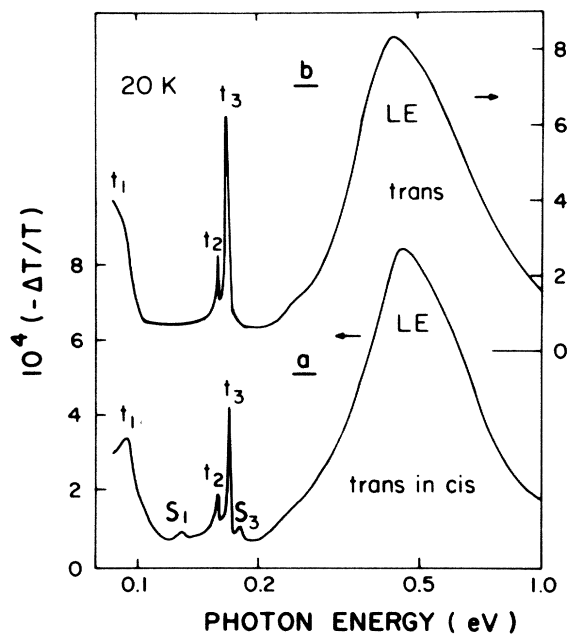


FIG. 1. Photoinduced absorption of (a) 30% *trans* in *cis*-(CH)_x, (b) fully isomerized *trans*-(CH)_x. t_1, t_2, t_3 are translational modes, S_1 and S_2 are additional modes. *LE* is the charged-soliton electronic transition.

20 K of the partially and fully isomerized (CH)_x samples is plotted up to 1 eV. Since *cis* chains do not have any induced ir activity,⁸ the induced absorption response of the partially isomerized sample is due to the *trans* chains. Both spectra contain a broad asymmetric band (*LE*), and three intense ir lines (t_1 , t_2 , and t_3); the *t(c)* spectrum contains, in addition, two weaker lines (S_1 and S_3). The *LE* band, which is the same in both *t(c)* and fully isomerized *trans*-(CH)_x, is due to electronic transitions^{8,9} from (to) photoinduced charged solitons (S^\pm). The three lines t_1 , t_2 , t_3 (Fig. 1) were identified earlier as *T* modes and were shown⁸ to correlate with the *LE* band. The higher *T*-mode frequencies in *t(c)* prove that the pinning³ of photogenerated S^\pm in *t(c)* is stronger than in *trans* samples; the stronger pinning slows down the S^\pm recombination kinetics as seen from the temperature and laser intensity dependence. In measurements extended up to 2.5 eV (not shown in Fig. 1) the PA spectra of the two samples continue to have similar structures, and we therefore identify the long-lived photocarriers in *t(c)* as charged solitons (S^\pm) as in *trans*-polyacetylene.^{9,12} The stronger pinning, however, indicates that S^\pm in *t(c)* are more confined. The new result here is the presence of the additional ir modes in *t(c)* [S_1 and S_3 in Fig. 1(a)] which demonstrates a qualitative change in the S^\pm properties due to the *cis* environment; as shown below this results from the shape modes.

The photoinduced vibrational ir absorption was measured with a 5-cm⁻¹ resolution and is shown in Fig. 2 on

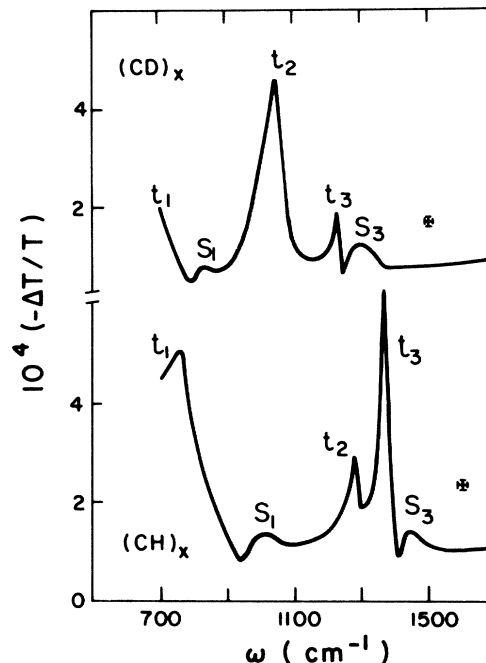


FIG. 2. Photoinduced absorption of the partially isomerized (~30% *trans*) (CH)_x and (CD)_x samples at 20 K showing the ir-active phonons in detail.

an enlarged scale for 30% *t(c)* (CH)_x and (CD)_x. The *T* modes in (CD)_x peak^{6,9} at ~400, 1045, and 1224 cm⁻¹ and their isotope shifts [compared to (CH)_x] are well understood.^{13,14} The additional asymmetric modes (S_1 and S_3 in Fig. 2) peak in (CH)_x at 1003 and 1426 cm⁻¹ and in (CD)_x at 835 and 1290 cm⁻¹; these frequencies shift downward upon isomerization. We found the *S* and *T* modes to have the same laser-intensity (I_L) and temperature dependences, implying that the same charged defect (S^\pm) is responsible for both. We therefore associate S_1 and S_3 in Fig. 2 with t_1 and t_3 , respectively. The frequencies, relative intensities, and widths of S_1 and S_3 were found to be given by the solution of $D_0(\omega) = -1.46$, where $D_0(\omega)$ is the same vibrational response function⁶ (for each isotope) which determines the Raman and the *T*-mode spectra.^{6,15} Using this $D_0(\omega)$ we estimate for the missing S_2 line $I_2^S/I_3^S < 0.1$, which is below our sensitivity. An additional feature of the PA spectra in Fig. 2 is the existence of pronounced dips in between each pair of *S* and *T* modes, for both isotopes. The dip frequencies are at 928 and 1405 cm⁻¹ in (CH)_x and at 798 and 1252 cm⁻¹ for (CD)_x; these frequencies correspond to the solutions of $D_0(\omega) = -1.36$ for both isotopes. Similarly to the *S* modes, the dips gradually disappear from the spectra upon isomerization and were not observed in fully isomerized samples. However, unlike the *S* modes, their frequencies do not change upon isomerization.

The twofold degeneracy of the *trans* backbone in *cis*-

rich samples is lifted because of short-chain effects or because of surrounding nondegenerate *cis* chains. This was proven independently by resonant Raman scattering (RRS) in $t(c)$ where the dispersion of the RRS lines with the laser frequency was shown to result from an extrinsic symmetry-breaking component in the Hamiltonian.¹¹ Under these conditions, intrinsic defects such as S^0 are pushed towards chain ends to reduce the potential energy; consequently long-lived S^\pm , which are mainly generated via^{12,15} $S^0 \mp e \rightarrow S^\pm$, also reside at the chain end. This explains the increased confinement that we have found for the photogenerated S^\pm in $t(c)$. Thus, the inversion symmetry of $t(c)$ chains containing S^0 is broken and modes are allowed to be simultaneously Raman and ir active. The disappearance of the additional S^\pm ir modes in $t(c)$ upon isomerization shows that they are not ir active for undisturbed solitons. Third-type ir-active soliton modes² (g_3) are therefore ruled out, and we propose that the additional S^\pm ir modes are due to the soliton shape modes which become ir active through a symmetry-breaking interaction with the soliton translational modes.

Without interaction, $\Delta\alpha(\omega)$ peaks⁶ at the three bare T modes whose frequencies are given by $D_0(\omega) = -(1 - \alpha_p)^{-1}$, where α_p is a pinning parameter.³ The three bare S modes have no ir activity,^{2,5} and their frequencies are given by $D_0(\omega) = -(1 - \gamma)^{-1}$, where γ is a parameter determined by the curvature of the soliton potential energy.⁵ When the S and T modes couple via a symmetry-breaking interaction $\sim B$, the effective Lagrangean for small oscillations is¹⁶

$$L_{\text{eff}} = L_\phi - e^2 A \dot{\phi} + L_\delta + B \delta(t) \phi(t), \quad (1)$$

where

$$L_\phi \sim \sum (\lambda_n / \lambda) [-\dot{\phi}_n^2 + (\dot{\phi}_n / \omega_n^0)^2] + (1 - \alpha_p) \dot{\phi}^2,$$

$$L_\delta \sim \sum (\lambda_n / \lambda) [-\dot{\delta}_n^2 + (\dot{\delta}_n / \omega_n^0)^2] + (1 - \gamma) \dot{\delta}^2;$$

λ_n , ϕ_n , and δ_n are the n th electron-phonon coupling, the translation-mode oscillation, and the shape-mode oscillation, respectively. In Eq. (1) $\sum \lambda_n = \lambda$, $\phi = \sum \phi_n$, $\delta = \sum \delta_n$, and A is the electromagnetic potential. The equations of motion (1) yield the conductivity $\sim \dot{\phi}(t)$ or the induced absorption $\Delta\alpha(\omega)$,

$$\Delta\alpha(\omega) \sim \omega [D_0^{-1}(\omega) + 1 - \gamma] / \{ [D_0^{-1}(\omega) + 1 - \alpha_p] [D_0^{-1}(\omega) + 1 - \gamma] - \beta \}, \quad (2)$$

where $\beta \sim B^2$. Equation (2) shows that for $\beta \neq 0$ the number of peaks in $\Delta\alpha(\omega)$ doubles; the poles of Eq. (2) occur at

$$D_0(\omega^\pm) = \frac{2 - \alpha_p - \gamma \pm [(\gamma - \alpha_p)^2 + 4\beta]^{1/2}}{(1 - \alpha_p)(1 - \gamma) - \beta}. \quad (3)$$

Equation (3) gives six mixed modes for polyacetylene which, for small β , can be separated into two distinct groups: three shape modes (+ sign) made ir active by the symmetry-breaking interaction, whose intensity scales linearly with β , and three translational modes (- sign). This explains the appearance of the additional set of ir-active modes in $t(c)$ and their decrease upon isomerization ($\beta \rightarrow 0$). Equation (3) shows that the S - and T -mode frequencies shift apart from the $\beta = 0$ value: The S -mode frequencies increase with β , while the T -mode frequencies decrease with β . This is in agreement with the apparent decrease of the S -mode frequencies upon isomerization. It also explains a surprising experimental correlation found between the T and S modes in $t(c)$: When we measured the PA spectrum with a faster chopping frequency f ($f = 1690$ Hz), we observed that t_3 decreased by 5 cm^{-1} (to 1367 cm^{-1}), while S_3 increased by 3 cm^{-1} and the ratio I_S^f/I_T^f dramatically increased. Similar repulsion of the S and T modes is observed upon increase of the laser intensity. These findings prove that an interaction binds the T and S modes together in agreement with our model. Such behavior is not likely to occur if the additional S modes were due to the third type (g_3) of ir bound modes of the soliton.² At higher f or at higher I_L we presumably measured photo-

generated S^\pm with shorter lifetime where the effect of the symmetry-breaking interaction is stronger.

A striking feature of Eq. (2) is the prediction of zeros in $\Delta\alpha(\omega)$ (where the numerator vanishes) at the three bare (i.e., undisturbed soliton) S -mode frequencies. This occurs in between each pair of T and S modes and accounts for the dips observed in the PA spectra (Fig. 2). Therefore, from the position of the observed dips and the appropriate $D_0(\omega)$ function^{6,14} we determine the three bare S -mode frequencies at 928 , 1286 , and 1405 cm^{-1} for $(\text{CH})_x$ and 798 , 1170 , and 1252 cm^{-1} for $(\text{CD})_x$; the bare S modes for both isotopes are given by $D_0(\omega) = -1.36$, i.e., $\gamma = 0.26$. The extended Raman-active modes are determined⁶ by $D_0(\omega) = -1 + 2\tilde{\lambda}$, where $2\tilde{\lambda} = 0.365$ at 80 K ; this gives for the ratio $\gamma/\tilde{\lambda} = 1.4$. This ratio is surprisingly close to the theoretical calculations^{1,2,5} which all neglect electron-electron interaction since then $\tilde{\lambda} = \lambda$. Using Eq. (3), the T -mode and the S -mode frequencies, and the derived value for γ , we calculate for the 30% $t(c)$ samples shown in Fig. 2 $\alpha_p = 0.16$ and $\beta = 0.008$.

The bare S modes of the soliton can, in principle, be directly observed as phonon sidebands accompanying the S^0 (S^\pm) optical transitions. Since the S^0 (S^\pm) transitions are allowed, their phonon sidebands should have *even* symmetry. However, these transitions are too weak and covered in $\alpha(\omega)$ by the much stronger interband transitions.¹⁷ This is not the case in optical modulation spectroscopy of S^0 ,^{15,18} since the interband transitions do not participate in it. The photoinduced bleaching of S^0

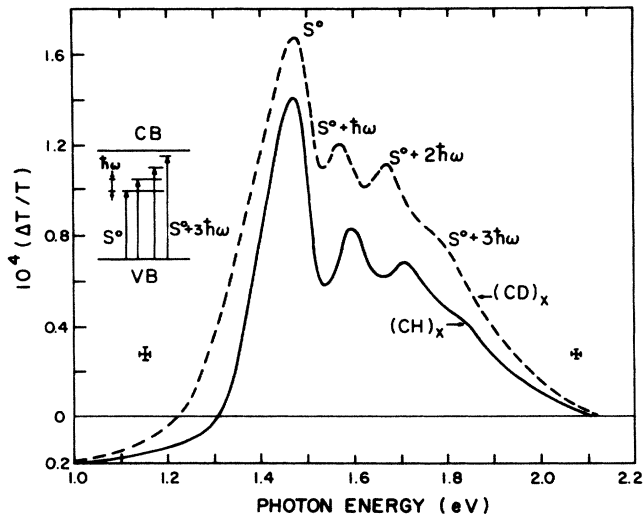


FIG. 3. Photoinduced transmission (PB) of *trans*-(CH)_x and -(CD)_x at 220 K; S^0 denotes optical transition to the neutral soliton level. $\hbar\omega$ is the phonon sideband energy; its correlated optical transitions with S^0 is shown in the inset.

in *trans*-(CH)_x and -(CD)_x at 220 K is shown in Fig. 3. The first peak in the spectrum was interpreted¹⁸ as the *o-o* transition of the S^0 ; at 220 K it peaks at 1.47 eV for both isotopes. The oscillations in the photoinduced bleaching spectrum with period of 920 cm⁻¹ in (CH)_x and 800 cm⁻¹ in (CD)_x were observed also in electro-modulation,¹⁹ thermal-modulation,¹⁹ doping-induced absorption,²⁰ and reflectivity measurements²¹ and were interpreted as due to electroabsorption of induced charges¹⁹ or as polaron transitions.²⁰ We found that the photoinduced oscillations, the peak at 1.47 eV (both seen in Fig. 3), and the PA peak at 0.5 eV (not shown in Fig. 3) share a common origin by virtue of the same dependence on I_L and on the temperature. Moreover, the oscillation period is exactly the lower bare S -mode frequency, for both isotopes, as derived from the dips in Fig. 2. These findings strongly indicate that the oscillations in the photoinduced spectrum are due to S -mode sidebands associated with S^0 optical transitions.

We note that we have not observed the third type of bound modes predicted² to be weakly ir active in the all-*trans* system. Our assignment for the new modes as

shape modes (second type of bound modes)^{2,5} is established by their dependence on *cis/trans* ratio (i.e., symmetry-breaking degree), laser intensity and chopping frequency, and the presence of dips and neutral-soliton sidebands. These results show that the observed modes are not of the third type² whose presence is yet to be observed in a more sensitive experiment.

At the Technion, this work was supported in part by the U.S.-Israel Binational Science Foundation and by the Israeli Academy for Basic Research, Jerusalem, Israel.

¹M. Nakahara and K. Maki, Phys. Rev. B **25**, 7789 (1982).

²H. Ito, A. Terai, Y. Ono, and Y. Wada, J. Phys. Soc. Jpn. **53**, 3519 (1984).

³B. Horovitz, Solid State Commun. **41**, 729 (1982).

⁴J. C. Hicks and G. A. Blaisdell, Phys. Rev. B **31**, 919 (1985).

⁵E. J. Mele and J. C. Hicks, Phys. Rev. B **32**, 2703 (1985), and Synth. Met. **13**, 149 (1986).

⁶B. Horovitz, Z. Vardeny, E. Ehrenfreund, and O. Brafman, Synth. Met. **9**, 215 (1984).

⁷E. J. Mele and M. J. Rice, Phys. Rev. Lett. **45**, 926 (1980).

⁸Z. Vardeny, J. Orenstein, and G. L. Baker, J. Phys. (Paris) **44**, C3-325 (1983), and Phys. Rev. Lett. **50**, 2032 (1983).

⁹G. B. Blanchet, C. R. Fincher, J. C. Chung, and A. J. Heeger, Phys. Rev. Lett. **50**, 1938 (1983).

¹⁰H. Kuzmany, E. A. Imhoff, D. B. Fitchen, and A. Sarhan-gi, Mol. Cryst. Liq. Cryst. **77**, 197 (1981).

¹¹Z. Vardeny, E. Ehrenfreund, O. Brafman, and B. Horovitz, Phys. Rev. Lett. **54**, 75 (1985).

¹²J. Orenstein, Z. Vardeny, G. L. Baker, G. Eagle, and S. Etemad, Phys. Rev. B **30**, 786 (1984).

¹³Z. Vardeny, J. Tanaka, H. Fujimoto, and M. Tanaka, Solid State Commun. **50**, 937 (1984).

¹⁴O. Brafman, Z. Vardeny, and E. Ehrenfreund, Solid State Commun. **53**, 615 (1985).

¹⁵Z. Vardeny, E. Ehrenfreund, and O. Brafman, Mol. Cryst. Liq. Cryst. **117**, 245 (1985).

¹⁶B. Horovitz *et al.*, to be published.

¹⁷B. R. Weinberger *et al.*, Phys. Rev. Lett. **53**, 86 (1984).

¹⁸Z. Vardeny and J. Tauc, Phys. Rev. Lett. **54**, 1844 (1985).

¹⁹J. Orenstein, G. L. Baker, and Z. Vardeny, J. Phys. (Paris), Colloq. **44**, C3-407 (1983).

²⁰S. Etemad *et al.*, J. Phys. (Paris), Colloq. **44**, C3-417 (1983).

²¹H. Eckhardt, J. Chem. Phys. **79**, 2085 (1983).